Measurement of beauty photoproduction using decays into muons in dijet events at HERA

To cite this article: ZEUS collaboration JHEP04(2009)133

View the article online for updates and enhancements.

Measurement of beauty photoproduction using decays into muons in dijet events at HERA

ZEUS collaboration

E-mail: tobias.haas@desy.de

ABSTRACT: Beauty photoproduction in dijet events has been measured at HERA with the ZEUS detector using an integrated luminosity of 126 pb^{-1}. Beauty was identified in events with a muon in the final state by using the transverse momentum of the muon relative to the closest jet. Lifetime information from the silicon vertex detector was also used; the impact parameter of the muon with respect to the primary vertex was exploited to discriminate between signal and background. Cross sections for beauty production as a function of the muon and the jet variables as well as dijet correlations are compared to QCD predictions and to previous measurements. The data are well described by predictions from next-to-leading-order QCD.

JHEP04(2009)133

Contents

1 Introduction

The production of beauty quarks in ep collisions should be accurately calculable in perturbative Quantum Chromodynamics (QCD) since the large mass of the b quark provides a hard scale. Therefore it is interesting to compare such predictions to results using photoproduction events where a low-virtuality photon, emitted by the incoming lepton, collides with a parton from the incoming proton. Previous photoproduction analyses presented by ZEUS used semi-leptonic decays into muons [1, 2] and electrons [3, 4], and found agreement with next-to-leading-order (NLO) QCD calculations and predictions based on the k_T factorisation approach [5]. Leptons from beauty decays were distinguished from other decay leptons and background by their large transverse momentum, $p_T^{\rm rel}$, relative to the axis of the jet with which they are associated.

For the analysis presented here, events with at least two jets (jj) were selected and b quarks were identified through their decay into muons with large $p_T^{\rm rel}$ and large impact parameter, δ, defined as the distance of closest approach of the muon with respect to the beam position. The latter was facilitated by the ZEUS silicon microvertex detector (MVD) [6]. The impact parameter is large for muons from b decays due to the long lifetime of B hadrons. A combination of the $p_T^{\rm rel}$ and δ methods was also used by the H1 collaboration [7] and good agreement was found with both the ZEUS results and the NLO QCD prediction, except for an excess at low p_T of the muon (p_T^{μ}) and jet (p_T^{j}). The measurement presented here covers a kinematic region extending to lower p_T^{μ} than the previous ZEUS and H1 jet measurements [1, 7]. The cross section for beauty production has

also been measured in $p\bar{p}$ collisions at the S$p\bar{p}$S [8–11] and Tevatron colliders [12–25] and in $\gamma\gamma$ interactions at LEP [26–28]. Most results are in good agreement with QCD predictions but large discrepancies are observed in some [26] of the results from $\gamma\gamma$ interactions at LEP.

The dijet sample of beauty photoproduction events was also used to study higher-order QCD topologies. At leading order (LO), the two jets in the event are produced back-to-back in azimuthal angle, such that $\Delta\phi^{jj} = \phi^{j1} - \phi^{j2} = \pi$. Additional soft radiation causes small azimuthal decorrelations, whilst $\Delta\phi^{jj}$ significantly lower than π is evidence of additional hard radiation. Dijet correlations have been previously measured at ZEUS in inclusive-jet and charm photoproduction at high transverse energies [29–31]; the conclusions from both are the same. Deviations from the NLO QCD predictions were found, especially in regions which are expected to be particularly sensitive to higher-order effects, i.e. at low $\Delta\phi^{jj}$. In this paper, the cross section versus $\Delta\phi^{jj}$ is presented for beauty photoproduction. These and other cross sections are compared to NLO QCD predictions and Monte Carlo models.

2   Experimental set-up

The analysis was performed with data taken in 2005 when HERA collided electrons with energy $E_e = 27.5$ GeV with protons of energy $E_p = 920$ GeV, resulting in a centre-of-mass energy of $\sqrt{s} = 318$ GeV. The results are based on an e^-p sample corresponding to an integrated luminosity of 125.9 ± 3.3 pb^{-1}.

A detailed description of the ZEUS detector can be found elsewhere [32]. A brief outline of the components that are most relevant for this analysis is given below.

In the kinematic range of the analysis, charged particles were tracked in the central tracking detector (CTD) [33–35] and the MVD [6]. These components operated in a magnetic field of 1.43 T provided by a thin superconducting solenoid. The CTD consisted of 72 cylindrical drift chamber layers, organised in nine superlayers covering the polar-angle[1] region $15° < \theta < 164°$. The MVD consisted of a barrel (BMVD) and a forward (FMVD) section with three cylindrical layers and four vertical planes of single-sided silicon strip sensors in the BMVD and FMVD respectively. The BMVD provided polar-angle coverage for tracks with three measurements from 30° to 150°. The FMVD extended the polar-angle coverage in the forward region to 7°. After alignment the single-hit resolution of the BMVD was 25 μm and the impact-parameter resolution of the CTD-BMVD system for high-momentum tracks was 100 μm.

The high-resolution uranium-scintillator calorimeter (CAL) [36–39] consisted of three parts: the forward (FCAL), the barrel (BCAL) and the rear (RCAL) calorimeters. Each part was subdivided transversely into towers and longitudinally into one electromagnetic section (EMC) and either one (in RCAL) or two (in BCAL and FCAL) hadronic sections (HAC). The smallest subdivision of the calorimeter was called a cell. The CAL energy res-

---

[1]The ZEUS coordinate system is a right-handed Cartesian system, with the Z axis pointing in the proton beam direction, referred to as the "forward direction", and the X axis pointing left towards the centre of HERA. The coordinate origin is at the nominal interaction point.

olutions, as measured under test-beam conditions, were $\sigma(E)/E = 0.18/\sqrt{E}$ for electrons and $\sigma(E)/E = 0.35/\sqrt{E}$ for hadrons (E in GeV).

The muon system consisted of rear, barrel (R/BMUON) and forward (FMUON) tracking detectors. The B/RMUON consisted of limited-streamer (LS) tube chambers placed behind the BCAL (RCAL), inside and outside a magnetised iron yoke surrounding the CAL. The barrel and rear muon chambers cover polar angles from $34°$ to $135°$ and from $135°$ to $171°$, respectively. The muon system exploited the magnetic field of the iron yoke and, in the forward direction, of two iron toroids magnetised to ~ 1.6 T to provide an independent measurement of the muon momentum.

The luminosity was measured using the Bethe-Heitler reaction $ep \rightarrow e\gamma p$ by a luminosity detector which consisted of independent lead-scintillator calorimeter [40–42] and magnetic spectrometer [43] systems. The fractional systematic uncertainty on the measured luminosity was 2.6%.

3 Data selection

The data were preselected by the ZEUS online trigger system [32, 44, 45] to contain two high-p_T jets and/or a muon candidate.

The hadronic system (including the muon) was reconstructed offline from energy-flow objects (EFOs) [46] which combine the information from calorimetry and tracking and which were corrected for dead material and for the presence of muons. Jets were reconstructed offline from EFOs using the k_T algorithm [47] in the longitudinally invariant mode [48]. The E-recombination scheme, which produces massive jets whose four-momenta are the sum of the four-momenta of the clustered objects, was used.

Muons were reconstructed by matching a track found in the CTD and the MVD with a track found in the inner chambers of the B/RMUON. Muons were associated with jets using the k_T algorithm; if the EFO corresponding to a reconstructed muon was included in a jet then the muon was considered to be associated with the jet, which will from now on be referred to as the muon-jet.

Events with one muon and two jets were selected by requiring:

- ≥ 1 muon with pseudorapidity $-1.6 < \eta^\mu < 1.3$, and transverse momentum $p_T^\mu > 2.5\,\text{GeV}$ (this cut was lowered to $p_T^\mu > 1.5\,\text{GeV}$ for the measurement of the differential cross section with respect to p_T^μ); the muon track was required to have at least 4 MVD hits;

- ≥ 2 jets with pseudorapidity $|\eta^j| < 2.5$, and transverse momentum $p_T^j > 7\,\text{GeV}$ for the highest-p_T^j jet and $p_T^j > 6\,\text{GeV}$ for the second-highest-p_T^j jet;

- that the muon was associated with a jet with $p_T^j > 6\,\text{GeV}$ which is not necessarily one of the two highest-p_T jets. To ensure a reliable p_T^{rel} measurement (see section 4), the residual jet transverse momentum, calculated excluding the associated muon, was required to be greater than $2\,\text{GeV}$;

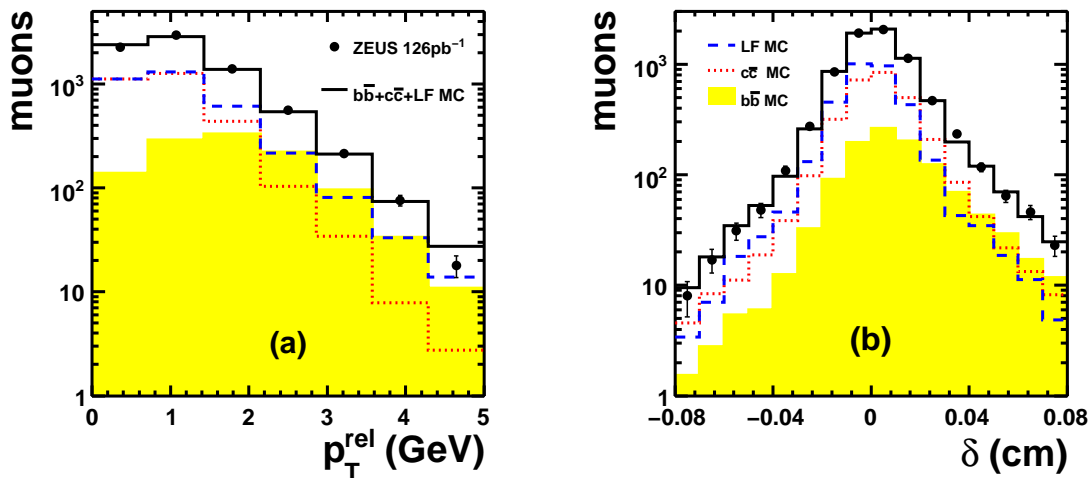- no scattered-electron candidate [49] found in the CAL;

ZEUS

Figure 1. Distributions of (a) p_T^{rel} and (b) δ. The data are compared to a mixture of beauty (shaded histogram), charm (dotted line) and light flavour(dashed line) PYTHIA MC samples, combined with the fractions given by the two-dimensional p_T^{rel}-δ fit. The total MC distribution is shown as the solid line.

- $0.2 < y_{\mathrm{JB}} < 0.8$, where y_{JB} is the estimator of the inelasticity, y, measured from the EFOs according to the Jacquet-Blondel method [50].

The last two cuts suppress the contributions from neutral current deep inelastic scattering events and from non-ep interactions. The total efficiency of all these selection cuts was $\sim 23\%$. A sample of 7351 events remained for $p_T^\mu > 2.5\,\mathrm{GeV}$ and 14172 events remained for $p_T^\mu > 1.5\,\mathrm{GeV}$.

4 Signal extraction

To evaluate detector acceptance and to provide the signal and background distributions, Monte Carlo (MC) samples of beauty, charm and light-flavour (LF) events were generated using PYTHIA 6.2 [51–53], corresponding respectively to 9, 4.5 and 1 times the luminosity of the data. The generated events were passed through a full simulation of the ZEUS detector based on GEANT 3.21 [54]. They were then subjected to the same trigger requirements and processed by the same reconstruction programs as the data.

Due to the large b-quark mass, muons from semi-leptonic beauty decays tend to be produced with high transverse momentum with respect to the direction of the jet containing the B hadron. The p_T^{rel} variable can therefore be exploited to extract the beauty signal; it is defined as:

$$p_T^{\mathrm{rel}} = \frac{|\mathbf{p}^\mu \times (\mathbf{p}^j - \mathbf{p}^\mu)|}{|\mathbf{p}^j - \mathbf{p}^\mu|}, \tag{4.1}$$

where $\mathbf{p}^\mu$ is the muon and $\mathbf{p}^j$ the jet momentum vector. An underestimation of the tails of the p_T^{rel} distribution in the background MC was corrected as described in a previous

– 4 –

publication [1]. The correction is applied in bins of p_T^{rel} to the LF MC sample. Half of the correction was also applied to the charm MC sample. The p_T^{rel} distribution for the selected data sample is compared to the MC simulation in figure 1(a).

Muons from semi-leptonic beauty decays tend to be produced at a secondary vertex, displaced from the primary vertex, because of the long lifetime of B hadrons. The signed impact parameter δ is calculated with respect to the beam position in the transverse plane (beam-spot). The beam-spot position was calculated every 2000 events as described elsewhere [55]. The sign of δ is positive if the muon intercepts the axis of the associated jet within the jet hemisphere; otherwise δ is negative.

The impact-parameter resolution in the MC was corrected [56], simultaneously taking into account the residual effects of multiple scattering and of the tracking resolution. The correction was extracted from inclusive-jet data by fitting the impact-parameter distribution with a double convolution of a Gaussian and a Breit-Wigner function. The widths of these functions were tuned taking into account the p_T dependence of the size of the correction.

Figure 1(b) shows the distribution of the reconstructed muon δ compared to predictions from the PYTHIA MC model for beauty, charm and LF events which were corrected as described above. The δ distribution for LF events, which is symmetric and peaked at zero, has a finite width which reflects the impact-parameter resolution. Whereas for beauty events, and to a lesser extent for charm events, the δ distribution is asymmetric towards positive δ.

The fractions of beauty $(a_{b\bar{b}})$ and charm $(a_{c\bar{c}})$ events in the sample were obtained from a three-component fit, f_μ, to the measured two-dimensional distributions of p_T^{rel} and δ:

$$f_\mu = a_{b\bar{b}} f_\mu^{b\bar{b}} + a_{c\bar{c}} f_\mu^{c\bar{c}} + (1 - a_{b\bar{b}} - a_{c\bar{c}}) f_\mu^{\mathrm{LF}}, \qquad (4.2)$$

where $f_\mu^{b\bar{b}}$, $f_\mu^{c\bar{c}}$ and f_μ^{LF} are the MC predicted shapes for beauty, charm and light flavour events. The fit used the minimum-χ^2 method and included MC statistical uncertainties. For differential cross sections the fit was repeated for each bin.

As an illustration, figure 2 shows the 68% probability contours from the two-dimensional fit described above and from one-dimensional fits carried out using p_T^{rel} or δ alone for the data sample with $p_T^\mu > 2.5\,\mathrm{GeV}$. Only statistical errors were taken into account. The two variables give complementary information. The p_T^{rel} fit alone is able to distinguish the b component from charm and LF but not to separate these two background components, while the δ fit gives a good determination of the total heavy quark fraction. The δ fit also provides a strong anti-correlation between the fractions of beauty and charm.[2] In the previous analysis [1], which used the p_T^{rel} method alone, the charm contribution was constrained to the charm cross section obtained from other measurements. This is not necessary here.

---

[2]Due to the correlations between p_T^{rel} and δ the combined contour is not completely contained within the overlap of the two individual contours.
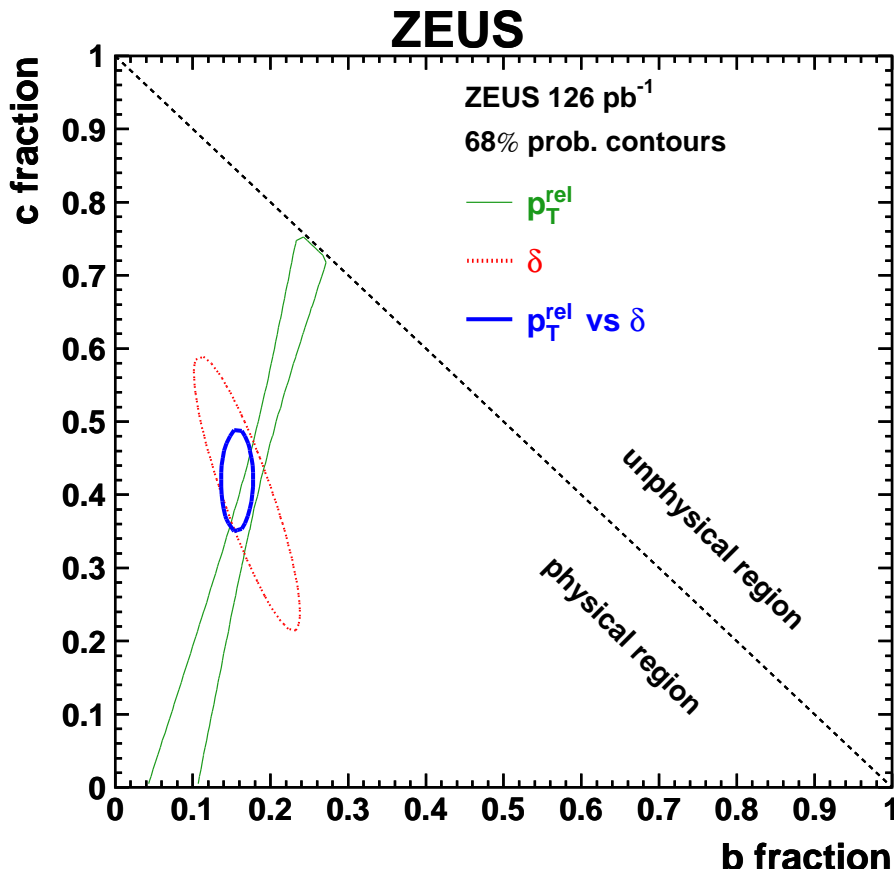
Figure 2. Contours of 68% probability in the plane defined by the beauty and the charm fractions. The result of the χ^2 fit to the two-dimensional $p_T^{\rm rel}$-δ distribution (thick solid line) and the one-dimensional distributions in $p_T^{\rm rel}$ (thin solid line) and δ (dotted line) are also shown. The diagonal line shows the boundary of the physical region in which the fractions of b, c and LF are positive.

5 Theoretical predictions and uncertainties

The measured cross sections are compared to NLO QCD predictions based on the FMNR [57] program. The parton distribution functions used for the nominal prediction were GRVG-HO [58] for the photon and CTEQ5M [59] for the proton. The b-quark mass was set to $m_b = 4.75$ GeV, and the renormalisation and factorisation scales to the transverse mass, $\mu_r = \mu_f = m_T = \sqrt{\frac{1}{2}\left((p_T^b)^2 + (p_T^{\bar{b}})^2\right) + m_b^2}$, where $p_T^{b(\bar{b})}$ is the transverse momentum of the b $(\bar{b})$ quark in the laboratory frame. Jets were reconstructed by running the k_T algorithm on the four-momenta of the b and $\bar{b}$ quarks and of the third light parton (if present) generated by the program. The fragmentation of the b quark into a B hadron was simulated by rescaling the quark three-momentum (in the frame in which $p_Z^b = -p_Z^{\bar{b}}$, obtained with a boost along Z) according to the Peterson [60] fragmentation function with $\epsilon = 0.0035$. The muon momentum was generated isotropically in the B-hadron rest frame from the decay spectrum given by PYTHIA which is in good

agreement with measurements made at B factories [61, 62].

The NLO cross sections, calculated for jets made of partons, were corrected for jet hadronisation effects to allow a direct comparison with the measured hadron-level cross sections. The correction factors, C_{had}, were derived from the MC simulation as the ratio of the hadron-level to the parton-level MC cross section, where the parton level is defined as being the result of the parton-showering stage of the simulation.

To evaluate the uncertainty on the NLO calculations, the b-quark mass and the renormalisation and factorisation scales were varied simultaneously to maximise the change, from $m_b = 4.5$ GeV and $\mu_r = \mu_f = m_T/2$ to $m_b = 5.0$ GeV and $\mu_r = \mu_f = 2m_T$, producing a variation in the cross section from $+34\%$ to -22%. The effect on the cross section of a variation of the Peterson parameter ϵ and of a change of the fragmentation function from the Peterson to the Kartvelishvili parameterisation was found in a previous publication [1] to be of the order of 3%. The effects of using different sets of parton densities and of a variation of the strong coupling constant were found to be within $\pm 4\%$. These effects are negligible with respect to that of a variation of the b-quark mass and the renormalisation and factorisation scales and are therefore not included. The uncertainty due to the hadronisation correction was also found to be negligible with respect to the dominant uncertainty.

The measured cross sections are also compared to the predictions of the PYTHIA 6.2 MC model scaled to the data. The predictions of PYTHIA were obtained [52] by mixing flavour-creation processes ($\gamma g \rightarrow b\bar{b}$, $gg \rightarrow b\bar{b}$, $q\bar{q} \rightarrow b\bar{b}$) calculated using massive matrix elements and the flavour-excitation (FE) processes ($bg \rightarrow bg$, $bq \rightarrow bq$), in which a heavy quark is extracted from the photon or proton parton density. The FE processes contribute about 27% to the total $b\bar{b}$ cross section. The small ($\sim 5\%$) [1] contribution from final-state gluon splitting in parton showers ($g \rightarrow b\bar{b}$) was not included. The parton density CTEQ5L [59] was used for the proton and GRVG-LO [58] for the photon; the b-quark mass was set to 4.75 GeV and the b-quark string fragmentation was performed according to the Peterson function with $\epsilon = 0.0041$ [60].

6   Systematic uncertainties

The main experimental uncertainties are calculated as follows (the resulting uncertainty on the total cross section is given in parentheses) [63]:

- the muon acceptance, including the efficiency of the muon chambers, of the reconstruction and of the B/RMUON matching to central tracks, is known to about 7%. An independent dimuon sample was analysed to determine this uncertainty based on a method [64] which has been repeated here ($\pm 7\%$);

- the error due to the uncertainty of the energy scale of the CAL was evaluated by varying the energy of the jets and the inelasticity y_{JB} in the MC by $\pm 3\%$ ($\pm 4\%$);

- the efficiency of finding a track with 4 MVD hits was measured in the data and in the MC. The ratio of the measured efficiencies was applied as a correction to the acceptance. The uncertainty on this ratio was included in the systematic uncertainty ($\pm 3\%$);
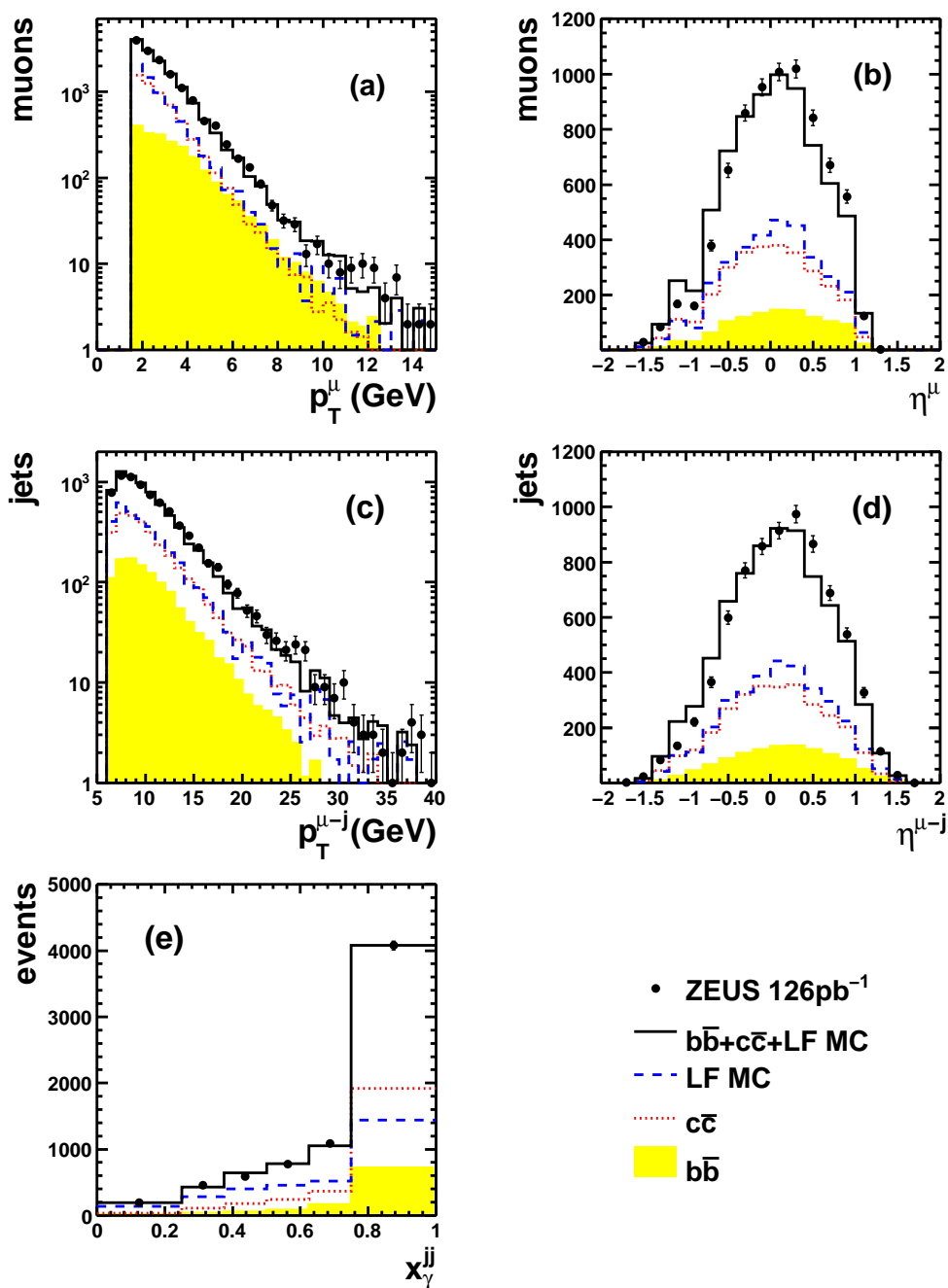
ZEUS

Figure 3. Distributions of (a) p_T^μ, (b) η^μ, (c) $p_T^{\mu-j}$, (d) $\eta^{\mu-j}$ and (e) x_γ^{jj}. The data are compared to a mixture of beauty (shaded histogram), charm (dotted line) and light flavour(dashed line) PYTHIA MC predictions, combined according to the fractions given by the two-dimensional $p_T^{\rm rel}$-δ fit. The total MC distribution is shown as the solid line. The kinematic region is restricted to $p_T^\mu > 1.5$ GeV ($p_T^\mu > 2.5$ GeV) for (a)((b)–(e)).

- the efficiency of the dijet trigger in the MC was corrected so that it reproduced the efficiency as measured in the data. The systematic uncertainty due to this correction was negligible;

- the MC η^μ distribution was reweighted in order to account for the differences (see figure 3) between data and MC ($< 1\%$);

- the uncertainty on the size of the correction to the shape of the impact-parameter distribution for the MC samples described in section 4 was evaluated by varying the widths of the Gaussian and Breit-Wigner distributions used in the correction function by $+20\%$ and -10% of their nominal values. These variations are such that the global MC distribution still provides a good description of the data ($^{+6\%}_{-10\%}$);

- the uncertainty on the p_T^{rel} shape of the LF and charm background was evaluated by:

  - varying the correction applied to the LF background by $\pm 20\%$ of its nominal value ($\pm 2\%$);

  - varying the p_T^{rel} shape of the charm component by removing or doubling the correction ($\pm 4\%$);

- the contribution of flavour-excitation events in PYTHIA was varied[3] by $+100\%/-50\%$ and simultaneously the contribution of $gg \rightarrow b\bar{b}$, $q\bar{q} \rightarrow b\bar{b}$ events was varied by $-50\%/+100\%$ ($\pm 4\%$); the contribution of $\gamma g \rightarrow b\bar{b}$ processes in PYTHIA was decreased by 20% and all other processes were increased by $+100\%$ ($\pm 2\%$).

The total systematic uncertainty was obtained by adding the above contributions in quadrature. A 2.6% overall normalisation uncertainty associated with the luminosity measurement was not included in the systematic uncertainty on the differential cross sections.

7 Results

Figure 3 shows the distributions of the kinematic variables of the muon p_T^μ and η^μ as well as those for the jet associated with the muon $p_T^{\mu-j}$ and $\eta^{\mu-j}$. The fraction x_γ^{jj} of the total hadronic $E - p_Z$ carried by the two highest-p_T jets[4] is given by:

$$x_\gamma^{jj} = \frac{\sum_{j=1,2}(E^j - p_Z^j)}{E - p_Z}. \tag{7.1}$$

The distribution of x_γ^{jj} is also shown in figure 3. The data are compared in shape to the MC simulations in which the relative contributions of beauty, charm and LF were mixed according to the fractions measured in this analysis as described in section 4. The

---

[3]The comparison between MC prediction and data for $d\sigma/dx_\gamma^{jj}$, see section 7, is still satisfactory for these variations.

[4]x_γ^{jj} is the massive-jets analogue of the x_γ^{obs} variable used for massless jets in other ZEUS publications [29].

p_T^μ range (GeV)	$d\sigma/dp_T^\mu \pm$ stat. $\pm$ syst. (pb/GeV)	C_{had}
1.5, 2.5	$41.05 \pm 7.74^{+8.26}_{-8.51}$	0.87
2.5, 4.0	$15.78 \pm 1.96^{+2.03}_{-1.98}$	0.93
4.0, 6.0	$4.87 \pm 1.03^{+0.69}_{-0.67}$	0.98
6.0, 10.0	$0.84 \pm 0.27^{+0.11}_{-0.11}$	1.01
η^μ range	$d\sigma/d\eta^\mu \pm$ stat. $\pm$ syst. (pb)	C_{had}
$-1.60, -0.75$	$3.86 \pm 1.37^{+1.40}_{-0.92}$	0.83
$-0.75, 0.25$	$16.81 \pm 2.30^{+2.34}_{-2.15}$	0.89
$0.25, 1.30$	$19.70 \pm 2.43^{+2.43}_{-3.09}$	0.92

Table 1. Differential muon cross section as a function of p_T^μ and η^μ. For further details see text. The multiplicative hadronisation correction, C_{had}, applied to the NLO prediction is shown in the last column.

comparison shows that the main features of the dijet-plus-muon sample are reasonably well reproduced by this MC mixture.

Total and differential visible cross sections have been measured for final states with at least one muon and two jets in the following kinematic region:

- $Q^2 < 1\,\mathrm{GeV}^2$ and $0.2 < y < 0.8$;

- $p_T^{j1,j2} > 7, 6\,\mathrm{GeV}$ and $|\eta^{j1,j2}| < 2.5$; the jets are defined as hadron-level jets using the k_T algorithm. For the purposes of jet-finding, B hadrons are treated as stable particles;

- $p_T^\mu > 2.5\,\mathrm{GeV}$ ($p_T^\mu > 1.5\,\mathrm{GeV}$ for $d\sigma/dp_T^\mu$) and $-1.6 < \eta^\mu < 1.3$;

- at least one muon is associated with a jet with $p_T^j > 6\,\mathrm{GeV}$. The muon is associated with the jet if it is the decay product of a B hadron contained in the jet, according to the k_T algorithm. Muons coming from both direct ($b \to \mu$) and indirect ($b \to c, \bar{c}, J/\Psi, \Psi' \to \mu$) decays are considered to be part of the signal.

The total visible cross section is

$$\sigma(ep \to eb\bar{b}X \to ejj\mu X') = 38.6 \pm 3.5(\mathrm{stat.})^{+4.6}_{-4.9}(\mathrm{syst.})\ \mathrm{pb}. \tag{7.2}$$

This result is compared to the NLO QCD calculation described in section 5. The prediction for the total visible cross section is

$$\sigma(ep \to ebbX \to ejj\mu X') = 37.0^{+11.9}_{-7.5}\ \mathrm{pb}, \tag{7.3}$$

in excellent agreement with the data.

Figure 4 and table 1 show the visible differential cross sections as a function of the muon transverse momentum and pseudorapidity. Also shown in figure 4 and in table 2 are

$p_T^{\mu\text{-}j}$ range (GeV)	$d\sigma/dp_T^{\mu\text{-}j} \pm$ stat. $\pm$ syst. (pb/GeV)	C_{had}
6, 11	$4.74 \pm 0.57^{+0.60}_{-0.59}$	0.89
11, 16	$1.78 \pm 0.32^{+0.24}_{-0.22}$	0.89
16, 30	$0.33 \pm 0.10^{+0.05}_{-0.05}$	0.92
$\eta^{\mu\text{-}j}$ range	$d\sigma/d\eta^{\mu\text{-}j} \pm$ stat. $\pm$ syst. (pb)	C_{had}
$-1.6, -0.6$	$6.13 \pm 1.41^{+1.50}_{-0.82}$	0.77
$-0.6,\ \ 0.4$	$13.89 \pm 2.20^{+2.08}_{-2.21}$	0.84
$0.4,\ \ 1.4$	$16.42 \pm 2.29^{+1.70}_{-2.29}$	0.99

Table 2. Differential cross section for jets associated with a muon as a function of $p_T^{\mu\text{-}j}$ and $\eta^{\mu\text{-}j}$. For further details see text.

x_γ^{jj} range	$d\sigma/dx_\gamma^{jj} \pm$ stat. $\pm$ syst. (pb)	C_{had}
0.000, 0.250	$11.85 \pm\ 4.96\ ^{+3.32}_{-2.40}$	0.69
0.250, 0.375	$17.17 \pm\ 7.89\ ^{+7.69}_{-4.47}$	0.78
0.375, 0.500	$14.81 \pm\ 7.56\ ^{+3.30}_{-4.06}$	0.86
0.500, 0.750	$22.19 \pm\ 4.48\ ^{+7.47}_{-4.51}$	0.86
0.750, 1.000	$106.63 \pm 12.63\ ^{+11.82}_{-12.74}$	0.92

Table 3. Differential cross section as a function of x_γ^{jj}. For further details see text.

the visible differential cross sections measured as a function of the transverse momentum of the jet associated with the muon $p_T^{\mu\text{-}j}$, and as a function of its pseudorapidity, $\eta^{\mu\text{-}j}$. The visible cross section as a function of p_T^μ is measured in the range $p_T^\mu > 1.5$ GeV, while the other cross sections are measured for $p_T^\mu > 2.5$ GeV. The NLO QCD predictions describe the data well and the PYTHIA MC also gives a good description of the shapes.

The visible differential cross section as a function of η^μ is also compared with a previous ZEUS measurement [1], which used the p_T^{rel} method to extract the beauty fraction. The two measurements agree well.[5]

Figure 5(a) and table 3 show the visible dijet cross section as a function of x_γ^{jj} (eq. (7.1)). The x_γ^{jj} variable corresponds at LO to the fraction of the exchanged-photon momentum entering the hard scattering process. In photoproduction, events can be classified into two types of process in LO QCD. In direct processes, the photon couples as a point-like object in the hard scatter. In resolved processes, the photon acts as a source of incoming partons, one of which takes part in the hard scatter. The x_γ^{jj} variable provides a tool to measure the relative importance of direct processes, which gives a peak at $x_\gamma^{jj} \sim 1$,

---

[5]The measurement presented by H1 [7] refers to a slightly different definition of the cross section and therefore cannot be compared to directly. However a qualitative comparison does not confirm their observation of an excess at low p_T^μ.
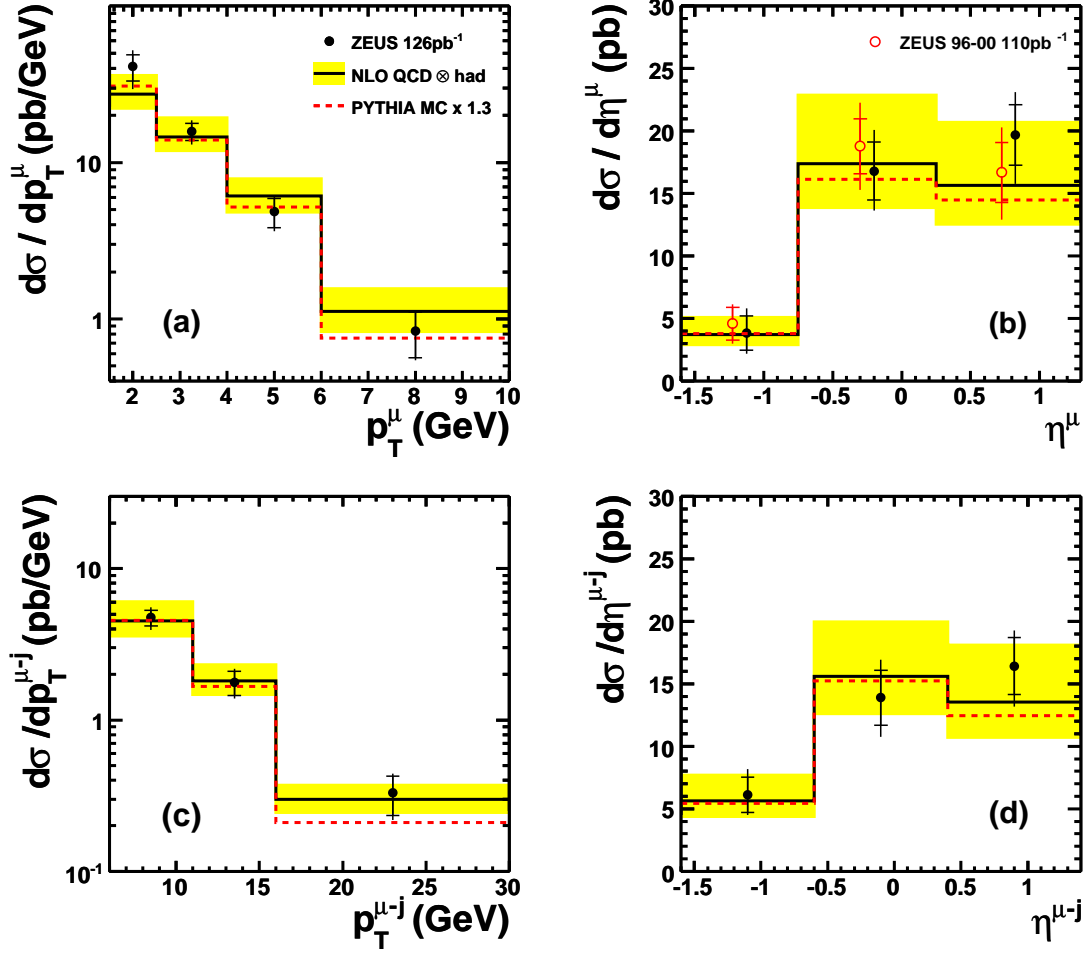
Figure 4. Differential cross section as a function (a) p_T^μ, (b) η^μ, (c) $p_T^{\mu-j}$ and (d) $\eta^{\mu-j}$ for $Q^2 < 1\,\text{GeV}^2$, $0.2 < y < 0.8$, $p_T^{j_1,j_2} > 7, 6\,\text{GeV}$, $|\eta_{j_1,j_2}| < 2.5$, and $-1.6 < \eta^\mu < 1.3$. For the p_T^μ cross section, the kinematic region is defined as $p_T^\mu > 1.5$ GeV and as $p_T^\mu > 2.5$ GeV for all other cross sections. The filled circles show the results from this analysis and the open circles show the results from the previous ZEUS measurement. The inner error bars are statistical uncertainties while the external bars show the statistical and systematic uncertainties added in quadrature. The band represents the NLO QCD predictions with their uncertainties. The PYTHIA MC predictions are also shown (dashed line).

and of resolved processes, which are distributed over the whole x_γ^{jj} range. The dominant contribution to the visible cross section comes from the high-x_γ^{jj} peak but a low-x_γ^{jj} component is also apparent. The NLO QCD prediction describes the measured visible cross section well. PYTHIA also gives a good description of the shape of the distribution.

Dijet angular correlations are particularly sensitive to higher-order effects and are therefore suitable to test the limitations of fixed-order perturbative QCD calculations.

ZEUS
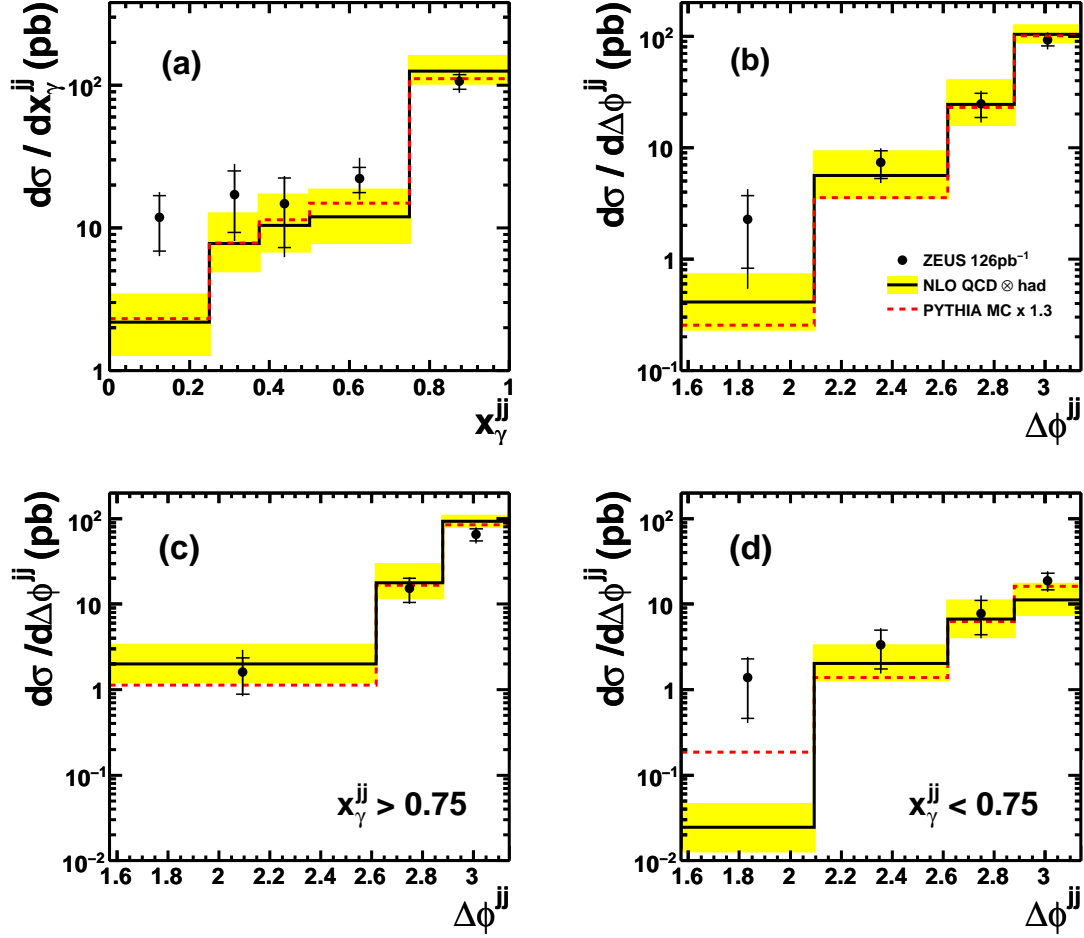
Figure 5. Differential cross sections as a function of (a) x_γ^{jj} and (b) $\Delta\phi^{jj}$ of the jet-jet system and $\Delta\phi^{jj}$ for (c) direct- and (d) resolved-enriched samples for $Q^2 < 1\,\mathrm{GeV}^2$, $0.2 < y < 0.8$, $p_T^{j_1,j_2} > 7, 6\,\mathrm{GeV}$, $\eta_{j_1,j_2} < 2.5$, $p_T^\mu > 2.5$ GeV and $-1.6 < \eta^\mu < 1.3$. The inner error bars are statistical uncertainties while the external bars show the statistical and systematic uncertainties added in quadrature. The band represents the NLO QCD predictions with their uncertainties. The PYTHIA MC predictions are also shown (dashed line).

The dijet variable measured, $\Delta\phi^{jj}$, was reconstructed from the two highest-p_T jets as:

$$\Delta\phi^{jj} = |\phi^{j1} - \phi^{j2}| \,. \tag{7.4}$$

In the FMNR program, at LO the differential cross section as a function of $\Delta\phi^{jj}$ is a delta function peaked at π. At NLO, exclusive three-jet production populates the region $\frac{2}{3}\pi < \Delta\phi^{jj} < \pi$, whilst smaller values of $\Delta\phi^{jj}$ require additional radiation such as a fourth jet in the event. An NLO QCD calculation can produce values of $\Delta\phi^{jj} < \frac{2}{3}\pi$ when the highest-p_T jet is not in the accepted kinematic region.

– 13 –

$\Delta\phi^{jj}$ range	$d\sigma/d\Delta\phi^{jj} \pm$ stat. $\pm$ syst. (pb)	C_{had}
$\frac{6\pi}{12}, \frac{8\pi}{12}$	$2.26\pm 1.44 \, ^{+1.34}_{-0.96}$	0.80
$\frac{8\pi}{12}, \frac{10\pi}{12}$	$7.35\pm 2.06 \, ^{+1.47}_{-1.45}$	0.79
$\frac{10\pi}{12}, \frac{11\pi}{12}$	$24.70\pm 6.04 \, ^{+4.66}_{-5.12}$	0.86
$\frac{11\pi}{12}, \frac{12\pi}{12}$	$92.91\pm11.10 \, ^{+10.46}_{-12.82}$	0.92

$x_\gamma^{jj} > 0.75$

$\Delta\phi^{jj}$ range	$d\sigma/d\Delta\phi^{jj} \pm$ stat. $\pm$ syst. (pb)	C_{had}
$\frac{6\pi}{12}, \frac{10\pi}{12}$	$1.62\pm 0.73 \, ^{+1.08}_{-0.27}$	0.82
$\frac{10\pi}{12}, \frac{11\pi}{12}$	$15.27\pm 4.75 \, ^{+2.50}_{-2.21}$	0.87
$\frac{11\pi}{12}, \frac{12\pi}{12}$	$65.69\pm10.66 \, ^{+8.14}_{-9.18}$	0.93

$x_\gamma^{jj} < 0.75$

$\Delta\phi^{jj}$ range	$d\sigma/d\Delta\phi^{jj} \pm$ stat. $\pm$ syst. (pb)	C_{had}
$\frac{6\pi}{12}, \frac{8\pi}{12}$	$1.38\pm0.92 \, ^{+0.46}_{-0.31}$	0.75
$\frac{8\pi}{12}, \frac{10\pi}{12}$	$3.36\pm1.60 \, ^{+0.97}_{-0.87}$	0.76
$\frac{10\pi}{12}, \frac{11\pi}{12}$	$7.75\pm3.37 \, ^{+3.67}_{-1.62}$	0.84
$\frac{11\pi}{12}, \frac{12\pi}{12}$	$18.84\pm4.17 \, ^{+3.71}_{-2.59}$	0.84

Table 4. Differential muon cross section as a function of $\Delta\phi^{jj}$ for all x_γ^{jj} and for $x_\gamma^{jj} > (<)0.75$. For further details see text.

The visible differential cross section as a function of $\Delta\phi^{jj}$ is shown in figure 5(b) and table 4. The NLO QCD predictions describe the data well. Visible cross sections as a function of $\Delta\phi^{jj}$ have also been measured separately for direct-enriched ($x_\gamma^{jj} > 0.75$) and resolved-enriched ($x_\gamma^{jj} < 0.75$) samples (figure 5(c) and (d)). The cross sections are well described by the NLO QCD prediction for $x_\gamma^{jj} > 0.75$ and for $x_\gamma^{jj} < 0.75$. The PYTHIA MC gives an equally good description of the shape of the distributions.

8 Conclusions

Beauty production identified through semi-leptonic decay into muons has been measured with the ZEUS detector in the kinematic range defined as: $Q^2 < 1\,\text{GeV}^2$; $0.2 < y < 0.8$; $p_T^{j1,j2} > 7, 6\,\text{GeV}$; $|\eta^{j1,j2}| < 2.5$; $p_T^\mu > 2.5\,\text{GeV}$; $-1.6 < \eta^\mu < 1.3$ with at least one muon being associated with a jet with $p_T^j > 6\,\text{GeV}$. Lifetime information was combined with the muon p_T^{rel} method to extract the fraction of beauty events in the data sample. Unlike the previous analysis, which used the p_T^{rel} method alone, it was not necessary to constrain the charm contribution to the charm cross section obtained from other measurements. The extracted charm contribution is consistent with expectation.

The total visible cross section was measured as well as visible differential cross sections as a function of the transverse momenta and pseudorapidities of the muon and of the jet

associated with the muon. The η^μ cross section was compared to the previous measurement. This analysis confirms the previous result with similar statistical precision and different sources of systematic uncertainty. Also, it was possible to measure the cross section as a function of the muon transverse momentum to $p_T^\mu > 1.5\,\text{GeV}$, a lower p_T^μ than in the previous muon-jet analysis. The p_T^μ cross section agrees well with the NLO QCD prediction and does not confirm the excess observed by H1 at low p_T^μ.

All results were compared to the PYTHIA MC model and to an NLO QCD prediction. The NLO QCD prediction describes the data well. The PYTHIA MC model also provides a good description of the shape of the distributions.

Beauty dijet angular-correlation cross sections were also measured. Separate measurements in direct-enriched and resolved-enriched regions were presented. The NLO QCD prediction describes the measured cross sections well.

Acknowledgments

Author list

S. Chekanov, M. Derrick, S. Magill, B. Musgrave, D. Nicholass,[1] J. Repond and R. Yoshida
Argonne National Laboratory, Argonne,
Illinois 60439-4815, U.S.A.[n]

M.C.K. Mattingly
Andrews University, Berrien Springs,
Michigan 49104-0380, U.S.A.

P. Antonioli, G. Bari, L. Bellagamba, D. Boscherini, A. Bruni, G. Bruni, F. Cindolo, M. Corradi, G. Iacobucci, A. Margotti, R. Nania and A. Polini
INFN Bologna,
Bologna, Italy[e]

S. Antonelli, M. Basile, M. Bindi, L. Cifarelli, A. Contin, S. De Pasquale,[2] G. Sartorelli and A. Zichichi
University and INFN Bologna,
Bologna, Italy[e]

D. Bartsch, I. Brock, H. Hartmann, E. Hilger, H.-P. Jakob, M. Jüngst, A.E. Nuncio-Quiroz, E. Paul, U. Samson, V. Schönberg, R. Shehzadi and M. Wlasenko
Physikalisches Institut der Universität Bonn,
Bonn, Germany[b]

N.H. Brook, G.P. Heath and J.D. Morris
H.H. Wills Physics Laboratory, University of Bristol,
Bristol, U.K.[m]

M. Kaur, P. Kaur[3] and I. Singh[3]
Panjab University, Department of Physics,
Chandigarh, India

M. Capua, S. Fazio, A. Mastroberardino, M. Schioppa, G. Susinno and E. Tassi
Calabria University, Physics Department and INFN,
Cosenza, Italy[e]

J.Y. Kim
Chonnam National University,
Kwangju, South Korea

Z.A. Ibrahim, F. Mohamad Idris, B. Kamaluddin and W.A.T. Wan Abdullah
Jabatan Fizik, Universiti Malaya,
50603 Kuala Lumpur, Malaysia[r]

Y. Ning, Z. Ren and F. Sciulli
Nevis Laboratories, Columbia University,
Irvington on Hudson, New York 10027, U.S.A.[o]

J. Chwastowski, A. Eskreys, J. Figiel, A. Galas, K. Olkiewicz, B. Pawlik, P. Stopa and L. Zawiejski
The Henryk Niewodniczanski Institute of Nuclear Physics, Polish Academy of Sciences,
Cracow, Poland[i]

L. Adamczyk, T. Bołd, I. Grabowska-Bołd, D. Kisielewska, J. Łukasik,[4] M. Przybycień and L. Suszycki
Faculty of Physics and Applied Computer Science,
AGH-University of Science and Technology,
Cracow, Poland[p]

A. Kotański[5] and W. Słomiński[6]
Department of Physics, Jagellonian University,

Cracow, Poland

O. Behnke, U. Behrens, C. Blohm, A. Bonato, K. Borras, D. Bot, R. Ciesielski,
N. Coppola, S. Fang, J. Fourletova,[7] A. Geiser, P. Göttlicher,[8] J. Grebenyuk,
I. Gregor, T. Haas, W. Hain, A. Hüttmann, F. Januschek, B. Kahle,
I.I. Katkov,[9] U. Klein,[10] U. Kötz, H. Kowalski, M. Lisovyi, E. Lobodzinska,
B. Löhr, R. Mankel,[11] I.-A. Melzer-Pellmann, S. Miglioranzi,[12] A. Monta-
nari, T. Namsoo, D. Notz,[11] A. Parenti, L. Rinaldi,[13] P. Roloff, I. Rubinsky,
U. Schneekloth, A. Spiridonov,[14] D. Szuba,[15] J. Szuba,[16] T. Theedt, J. Ukleja,[17]
G. Wolf, K. Wrona, A.G. Yagües Molina, C. Youngman and W. Zeuner[11]
Deutsches Elektronen-Synchrotron DESY,
Hamburg, Germany

V. Drugakov, W. Lohmann and S. Schlenstedt
Deutsches Elektronen-Synchrotron DESY,
Zeuthen, Germany

G. Barbagli and E. Gallo
INFN Florence,
Florence, Italy[e]

P.G. Pelfer
University and INFN Florence,
Florence, Italy[e]

A. Bamberger, D. Dobur, F. Karstens and N.N. Vlasov[18]
Fakultät für Physik der Universität Freiburg i.Br.,
Freiburg i.Br., Germany[b]

P.J. Bussey,[19] A.T. Doyle, W. Dunne, M. Forrest, M. Rosin, D.H. Saxon and
I.O. Skillicorn
Department of Physics and Astronomy, University of Glasgow,
Glasgow, U.K.[m]

I. Gialas[20] and K. Papageorgiu
Department of Engineering in Management and Finance, Univ. of Aegean,
Greece

U. Holm, R. Klanner, E. Lohrmann, H. Perrey, P. Schleper, T. Schörner-
Sadenius, J. Sztuk, H. Stadie and M. Turcato
Hamburg University, Institute of Exp. Physics,
Hamburg, Germany[b]

C. Foudas, C. Fry, K.R. Long and A.D. Tapper

Imperial College London, High Energy Nuclear Physics Group,
London, U.K.[m]

T. Matsumoto, K. Nagano, K. Tokushuku,[21] S. Yamada and Y. Yamazaki[22]

Institute of Particle and Nuclear Studies, KEK,
Tsukuba, Japan[f]

A.N. Barakbaev, E.G. Boos, N.S. Pokrovskiy and B.O. Zhautykov

Institute of Physics and Technology of Ministry of Education and Science of Kazakhstan,
Almaty, Kazakhstan

V. Aushev,[23] O. Bachynska, M. Borodin, I. Kadenko, A. Kozulia, V. Libov,
D. Lontkovskyi, I. Makarenko, Iu. Sorokin, A. Verbytskyi and O. Volynets

Institute for Nuclear Research,
National Academy of Sciences and Kiev National University,
Kiev, Ukraine

D. Son

Kyungpook National University, Center for High Energy Physics,
Daegu, South Korea[g]

J. de Favereau and K. Piotrzkowski

Institut de Physique Nucléaire, Université Catholique de Louvain,
Louvain-la-Neuve, Belgium[q]

F. Barreiro, C. Glasman, M. Jimenez, L. Labarga, J. del Peso, E. Ron,
M. Soares, J. Terrón and C. Uribe-Estrada

Departamento de Física Teórica, Universidad Autónoma de Madrid,
Madrid, Spain[l]

F. Corriveau, C. Liu, J. Schwartz, R. Walsh and C. Zhou

Department of Physics, McGill University,
Montréal, Québec, H3A 2T8, Canada[a]

T. Tsurugai

Meiji Gakuin University, Faculty of General Education,
Yokohama, Japan[f]

A. Antonov, B.A. Dolgoshein, D. Gladkov, V. Sosnovtsev, A. Stifutkin and
S. Suchkov

Moscow Engineering Physics Institute,

Moscow, Russia[j]

R.K. Dementiev, P.F. Ermolov,[†] L.K. Gladilin, Yu.A. Golubkov, L.A. Khein, I.A. Korzhavina, V.A. Kuzmin, B.B. Levchenko,[24] O.Yu. Lukina, A.S. Proskuryakov, L.M. Shcheglova and D.S. Zotkin
Moscow State University, Institute of Nuclear Physics,
Moscow, Russia[k]

I. Abt, A. Caldwell, D. Kollar, B. Reisert and W.B. Schmidke
Max-Planck-Institut für Physik,
München, Germany

G. Grigorescu, A. Keramidas, E. Koffeman, P. Kooijman, A. Pellegrino, H. Tiecke, M. Vázquez[12] and L. Wiggers
NIKHEF and University of Amsterdam,
Amsterdam, Netherlands[h]

N. Brümmer, B. Bylsma, L.S. Durkin, A. Lee and T.Y. Ling
Physics Department, Ohio State University,
Columbus, Ohio 43210, U.S.A.[n]

P.D. Allfrey, M.A. Bell, A.M. Cooper-Sarkar, R.C.E. Devenish, J. Ferrando, B. Foster, C. Gwenlan,[25] K. Horton,[26] K. Oliver, A. Robertson and R. Walczak
Department of Physics, University of Oxford,
Oxford, U.K.[m]

A. Bertolin, F. Dal Corso, S. Dusini, A. Longhin and L. Stanco
INFN Padova,
Padova, Italy[e]

P. Bellan, R. Brugnera, R. Carlin, A. Garfagnini and S. Limentani
Dipartimento di Fisica dell' Università and INFN,
Padova, Italy[e]

B.Y. Oh, A. Raval and J.J. Whitmore[27]
Department of Physics, Pennsylvania State University,
University Park, Pennsylvania 16802, U.S.A.[o]

Y. Iga
Polytechnic University,
Sagamihara, Japan[f]

G. D'Agostini, G. Marini and A. Nigro
Dipartimento di Fisica, Università 'La Sapienza' and INFN,
Rome, Italy[e]

J.E. Cole[28] and J.C. Hart
Rutherford Appleton Laboratory, Chilton,
Didcot, Oxon, U.K.[m]

H. Abramowicz,[29] R. Ingbir, S. Kananov, A. Levy and A. Stern
Raymond and Beverly Sackler Faculty of Exact Sciences,
School of Physics, Tel Aviv University,
Tel Aviv, Israel[d]

M. Kuze and J. Maeda
Department of Physics, Tokyo Institute of Technology,
Tokyo, Japan[f]

R. Hori, S. Kagawa,[30] N. Okazaki, S. Shimizu and T. Tawara
Department of Physics, University of Tokyo,
Tokyo, Japan[f]

R. Hamatsu, H. Kaji,[31] S. Kitamura,[32] O. Ota[33] and Y.D. Ri
Tokyo Metropolitan University, Department of Physics,
Tokyo, Japan[f]

M. Costa, M.I. Ferrero, V. Monaco, R. Sacchi, V. Sola and A. Solano
Università di Torino and INFN,
Torino, Italy[e]

M. Arneodo and M. Ruspa
Università del Piemonte Orientale,
Novara, Italy and
INFN,
Torino, Italy[e]

S. Fourletov,[7] J.F. Martin and T.P. Stewart
Department of Physics, University of Toronto,
Toronto, Ontario, M5S 1A7, Canada[a]

S.K. Boutle,[20] J.M. Butterworth, R. Hall-Wilton,[34] T.W. Jones, J.H. Loizides and M. Wing[35]
Physics and Astronomy Department, University College London,

London, U.K.^{m}

B. Brzozowska, J. Ciborowski,^{36} G. Grzelak, P. Kulinski, P. Łużniak,^{37} J. Malka,^{37} R.J. Nowak, J.M. Pawlak, W. Perlanski,^{37} T. Tymieniecka^{38} and A.F. Żarnecki
Warsaw University, Institute of Experimental Physics,
Warsaw, Poland

M. Adamus, P. Plucinski^{39} and A. Ukleja
Institute for Nuclear Studies,
Warsaw, Poland

Y. Eisenberg, D. Hochman and U. Karshon
Department of Particle Physics, Weizmann Institute,
Rehovot, Israel^c

E. Brownson, D.D. Reeder, A.A. Savin, W.H. Smith and H. Wolfe
Department of Physics, University of Wisconsin,
Madison, Wisconsin 53706, U.S.A.^{n}

S. Bhadra, C.D. Catterall, Y. Cui, G. Hartner, S. Menary, U. Noor, J. Standage and J. Whyte
Department of Physics, York University,
Ontario, M3J1P3, Canada^a

^{1}*also affiliated with University College London, U.K.*
^{2}*now at University of Salerno, Italy*
^{3}*also working at Max Planck Institute, Munich, Germany*
^{4}*now at Institute of Aviation, Warsaw, Poland*
^{5}*supported by the research grant no. 1 P03B 04529 (2005-2008)*
^{6}*This work was supported in part by the Marie Curie Actions Transfer of Knowledge project COCOS (contract MTKD-CT-2004-517186)*
^{7}*now at University of Bonn, Germany*
^{8}*now at DESY group FEB, Hamburg, Germany*
^{9}*also at Moscow State University, Russia*
^{10}*now at University of Liverpool, U.K.*
^{11}*on leave of absence at CERN, Geneva, Switzerland*
^{12}*now at CERN, Geneva, Switzerland*
^{13}*now at Bologna University, Bologna, Italy*
^{14}*also at Institut of Theoretical and Experimental Physics, Moscow, Russia*
^{15}*also at INP, Cracow, Poland*
^{16}*also at FPACS, AGH-UST, Cracow, Poland*
^{17}*partially supported by Warsaw University, Poland*

References

[1] ZEUS collaboration, S. Chekanov et al., *Beauty photoproduction measured using decays into muons in dijet events in ep collisions at $\sqrt{s} = 318\,GeV$, Phys. Rev.* **D 70** (2004) 012008 [*Erratum ibid.* **D 74** (2006) 059906] [hep-ex/0312057] [SPIRES].

[2] ZEUS collaboration, S. Chekanov et al., *Measurement of beauty production from dimuon events at HERA*, preprint DESY-08-129, [*JHEP* **02** (2009) 032] [arXiv:0811.0894] [SPIRES].

[3] ZEUS collaboration, J. Breitweg et al., *Measurement of open beauty production in photoproduction at HERA, Eur. Phys. J.* **C 18** (2001) 625 [hep-ex/0011081] [SPIRES].

[4] ZEUS collaboration, S. Chekanov et al., *Beauty photoproduction using decays into electrons at HERA, Phys. Rev.* **D 78** (2008) 072001 [arXiv:0805.4390] [SPIRES].

[5] A.V. Lipatov and N.P. Zotov, *Beauty photoproduction at HERA: k_T-factorization versus experimental data, Phys. Rev.* **D 73** (2006) 114018 [hep-ph/0601240] [SPIRES].

[6] ZEUS collaboration, A. Polini et al., *The design and performance of the ZEUS micro vertex detector, Nucl. Inst. Meth.* **A 581** (2007) 656 [arXiv:0708.3011] [SPIRES].

[7] H1 collaboration, A. Aktas et al., *Measurement of beauty production at HERA using events with muons and jets, Eur. Phys. J.* **C 41** (2005) 453 [hep-ex/0502010] [SPIRES].

[8] UA1 collaboration, C. Albajar et al., *Beauty production at the CERN $p\bar{p}$ collider. 1, Phys. Lett.* **B 186** (1987) 237 [SPIRES].

[9] UA1 collaboration, C. Albajar et al., *Measurement of the bottom quark production cross-section in $p\bar{p}$ collisions at $\sqrt{s} = 0.63\,TeV$, Phys. Lett.* **B 213** (1988) 405 [SPIRES].

[10] UA1 collaboration, C. Albajar et al., *Beauty production at the CERN $p\bar{p}$ collider, Phys. Lett.* **B 256** (1991) 121 [*Erratum ibid.* **B 262** (1991) 497] [SPIRES].

[11] UA1 collaboration, C. Albajar et al., *Measurement of $b\bar{b}$ correlations at the CERN $p\bar{p}$ collider, Z. Phys.* **C 61** (1994) 41 [SPIRES].

[12] CDF collaboration, F. Abe et al., *Measurement of the bottom quark production cross-section using semileptonic decay electrons in $p\bar{p}$ collisions at $\sqrt{s} = 1.8\,TeV$, Phys. Rev. Lett.* **71** (1993) 500 [SPIRES].

[13] CDF collaboration, F. Abe et al., *Measurement of bottom quark production in 1.8 TeV pp̄ collisions using semileptonic decay muons*, *Phys. Rev. Lett.* **71** (1993) 2396 [SPIRES].

[14] CDF collaboration, F. Abe et al., *Measurement of the B meson differential cross-section, dσ/dp_T, in pp̄ collisions at √s = 1.8 TeV*, *Phys. Rev. Lett.* **75** (1995) 1451 [hep-ex/9503013] [SPIRES].

[15] CDF collaboration, F. Abe et al., *Measurement of correlated μ − b̄ jet cross-sections in pp̄ collisions at √s = 1.8 TeV*, *Phys. Rev.* **D 53** (1996) 1051 [hep-ex/9508017] [SPIRES].

[16] CDF collaboration, F. Abe et al., *Measurement of bb̄ production correlations, B⁰B̄⁰ mixing and a limit on ε(B) in pp̄ collisions at √s = 1.8 TeV*, *Phys. Rev.* **D 55** (1997) 2546 [SPIRES].

[17] CDF collaboration, D.E. Acosta et al., *Measurement of the B⁺ total cross section and B⁺ differential cross section dσ/dp_T in pp̄ collisions at √s = 1.8 TeV*, *Phys. Rev.* **D 65** (2002) 052005 [hep-ph/0111359] [SPIRES].

[18] CDF collaboration, D.E. Acosta et al., *Measurement of the ratio of b quark production cross sections in p̄p collisions at √s = 630 GeV and √s = 1800 GeV*, *Phys. Rev.* **D 66** (2002) 032002 [hep-ex/0206019] [SPIRES].

[19] CDF collaboration, D.E. Acosta et al., *Measurement of the J/ψ meson and b-hadron production cross sections in pp̄ collisions at √s = 1960 GeV*, *Phys. Rev.* **D 71** (2005) 032001 [hep-ex/0412071] [SPIRES].

[20] CDF collaboration, D.E. Acosta et al., *Measurements of bb̄ azimuthal production correlations in pp̄ collisions at √s = 1.8 TeV*, *Phys. Rev.* **D 71** (2005) 092001 [hep-ex/0412006] [SPIRES].

[21] CDF collaboration, T. Aaltonen et al., *Measurement of correlated b⁻b̄ production in p⁻p̄ collisions at √s = 1960 GeV*, *Phys. Rev.* **D 77** (2008) 072004 [arXiv:0710.1895] [SPIRES].

[22] D0 collaboration, S. Abachi et al., *Inclusive μ and B quark production cross-sections in pp̄ collisions at √s = 1.8 TeV*, *Phys. Rev. Lett.* **74** (1995) 3548 [SPIRES].

[23] D0 collaboration, B. Abbott et al., *The bb̄ production cross section and angular correlations in pp̄ collisions at √s = 1.8 TeV*, *Phys. Lett.* **B 487** (2000) 264 [hep-ex/9905024] [SPIRES].

[24] D0 collaboration, B. Abbott et al., *Small angle muon and bottom quark production in pp̄ collisions at √s = 1.8 TeV*, *Phys. Rev. Lett.* **84** (2000) 5478 [hep-ex/9907029] [SPIRES].

[25] D0 collaboration, B. Abbott et al., *Cross section for b jet production in p̄p collisions at √s = 1.8 TeV*, *Phys. Rev. Lett.* **85** (2000) 5068 [hep-ex/0008021] [SPIRES].

[26] L3 collaboration, M. Acciarri et al., *Measurements of the cross-sections for open charm and beauty production in γγ collisions at √s = 189 GeV to 202 GeV*, *Phys. Lett.* **B 503** (2001) 10 [hep-ex/0011070] [SPIRES].

[27] L3 collaboration, P. Achard et al., *Measurement of the cross section for open-beauty production in photon-photon collisions at LEP*, *Phys. Lett.* **B 619** (2005) 71 [hep-ex/0507041] [SPIRES].

[28] ALEPH collaboration, S. Schael et al., *Measurement of the cross section for open b-quark production in two-photon interactions at LEP*, *JHEP* **09** (2007) 102 [arXiv:0706.3150] [SPIRES].

[29] ZEUS collaboration, S. Chekanov et al., *Inclusive jet cross sections and dijet correlations in D*± photoproduction at HERA*, *Nucl. Phys.* **B 729** (2005) 492 [hep-ex/0507089] [SPIRES].

[30] ZEUS collaboration, S. Chekanov et al., *High-E_T dijet photoproduction at HERA*, *Phys. Rev.* **D 76** (2007) 072011 [`arXiv:0706.3809`] [SPIRES].

[31] ZEUS collaboration, S. Chekanov et al., *Dijet angular distributions in photoproduction of charm at HERA*, *Phys. Lett.* **B 565** (2003) 87 [`hep-ex/0302025`] [SPIRES].

[32] ZEUS collaboration, U. Holm, *The ZEUS detector*, status report, unpublished, DESY, Germany (1993), available on http://www-zeus.desy.de/bluebook/bluebook.html.

[33] N. Harnew et al., *Vertex triggering using time difference measurements in the ZEUS central tracking detector*, *Nucl. Inst. Meth.* **A 279** (1989) 290 [SPIRES].

[34] B. Foster et al., *The performance of the ZEUS central tracking detector z-by-timing electronics in a transputer based data acquisition system*, *Nucl. Phys. Proc. Suppl.* **B 32** (1993) 181 [SPIRES].

[35] ZEUS collaboration, B. Foster et al., *The design and construction of the ZEUS central tracking detector*, *Nucl. Inst. Meth.* **A 338** (1994) 254 [SPIRES].

[36] M. Derrick et al., *Design and construction of the ZEUS barrel calorimeter*, *Nucl. Inst. Meth.* **A 309** (1991) 77 [SPIRES].

[37] ZEUS CALORIMETER GROUP collaboration and ZEUS collaboration, A. Andresen et al., *Construction and beam test of the ZEUS forward and rear calorimeter*, *Nucl. Inst. Meth.* **A 309** (1991) 101 [SPIRES].

[38] A. Caldwell et al., *Design and implementation of a high precision readout system for the ZEUS calorimeter*, *Nucl. Inst. Meth.* **A 321** (1992) 356 [SPIRES].

[39] ZEUS BARREL CALORIMETER GROUP collaboration, A. Bernstein et al., *Beam tests of the ZEUS barrel calorimeter*, *Nucl. Inst. Meth.* **A 336** (1993) 23 [SPIRES].

[40] ZEUS LUMINOSITY MONITOR GROUP collaboration, J. Andruszków et al., *First measurement of HERA luminosity by ZEUS lumi monitor*, Preprint DESY-92-066, DESY, Germany (1992) [SPIRES].

[41] ZEUS collaboration, M. Derrick et al., *Measurement of total and partial photon proton cross-sections at 180 GeV center-of-mass energy*, *Z. Phys.* **C 63** (1994) 391 [SPIRES].

[42] ZEUS LUMINOSITY GROUP collaboration, J. Andruszków et al., *Luminosity measurement in the ZEUS experiment*, *Acta Phys. Pol.* **B 32** (2001) 2025 [SPIRES].

[43] M. Helbich et al., *The spectrometer system for measuring ZEUS luminosity at HERA*, *Nucl. Inst. Meth.* **A 565** (2006) 572 [`physics/0512153`] [SPIRES].

[44] P.D. Allfrey et al., *The design and performance of the ZEUS global tracking trigger*, *Nucl. Inst. Meth.* **A 580** (2007) 1257 [SPIRES].

[45] W.H. Smith, K. Tokushuku and L.W. Wiggers, *The ZEUS trigger system*, in *Proceedings of Computing in High-Energy Physics (CHEP), Annecy France September* 1992, C. Verkerk and W. Wojcik eds., CERN, Geneva Switzerland (1992), pg. 222 [DESY-92-150B] [SPIRES].

[46] G.M. Briskin, *Diffractive dissociation in ep deep inelastic scattering*, Ph.D. thesis, report DESY-THESIS-1998-036, Tel Aviv University, Israel (1998) [SPIRES].

[47] S. Catani, Y.L. Dokshitzer, M.H. Seymour and B.R. Webber, *Longitudinally invariant K_t clustering algorithms for hadron hadron collisions*, *Nucl. Phys.* **B 406** (1993) 187 [SPIRES].

[48] S.D. Ellis and D.E. Soper, *Successive combination jet algorithm for hadron collisions*, *Phys. Rev.* **D 48** (1993) 3160 [`hep-ph/9305266`] [SPIRES].

[49] H. Abramowicz, A. Caldwell and R. Sinkus, *Neural network based electron identification in the ZEUS calorimeter*, *Nucl. Inst. Meth.* **A 365** (1995) 508 [hep-ex/9505004] [SPIRES].

[50] F. Jacquet and A. Blondel, *Detection of the charged current event — method II*, in *Proceedings of the Study for an ep facility for Europe*, U. Amaldi (ed.), Hamburg Germany (1979), pg. 391 [DESY-79-48] [SPIRES].

[51] T. Sjöstrand et al., *High-energy-physics event generation with PYTHIA* 6.1, *Comput. Phys. Commun.* **135** (2001) 238 [hep-ph/0010017] [SPIRES].

[52] E. Norrbin and T. Sjöstrand, *Production and hadronization of heavy quarks*, *Eur. Phys. J.* **C 17** (2000) 137 [hep-ph/0005110] [SPIRES].

[53] T. Sjöstrand, L. Lönnblad and S. Mrenna, *PYTHIA* 6.2*: physics and manual*, hep-ph/0108264 [SPIRES].

[54] R. Brun et al., GEANT3, Technical Report CERN-DD/EE/84-1, CERN Geneva Switzerland (1987).

[55] D. Nicholass, *The study of $D^{\pm}$ and D^0 meson production in deep inelastic scattering at HERA II with the ZEUS detector*, Ph.D. Thesis, report DESY-THESIS-2008-046, University College London, London U.K. (2008) [SPIRES].

[56] S. Miglioranzi, *Beauty photoproduction at HERA II with the ZEUS experiment*, Ph.D. Thesis, unpublished, University College London, London U.K. (2006) [SPIRES].

[57] S. Frixione, M.L. Mangano, P. Nason and G. Ridolfi, *Heavy quark correlations in photon-hadron collisions*, *Nucl. Phys.* **B 412** (1994) 225 [hep-ph/9306337] [SPIRES].

[58] M. Gluck, E. Reya and A. Vogt, *Photonic parton distributions*, *Phys. Rev.* **D 46** (1992) 1973 [SPIRES].

[59] CTEQ collaboration, H.L. Lai et al., *Global QCD analysis of parton structure of the nucleon: cTEQ5 parton distributions*, *Eur. Phys. J.* **C 12** (2000) 375 [hep-ph/9903282] [SPIRES].

[60] C. Peterson, D. Schlatter, I. Schmitt and P.M. Zerwas, *Scaling violations in inclusive e^+e^- annihilation spectra*, *Phys. Rev.* **D 27** (1983) 105 [SPIRES].

[61] BELLE collaboration, K. Abe et al., *Measurement of the inclusive semileptonic branching fraction of B mesons and $|V_{cb}|$*, *Phys. Lett.* **B 547** (2002) 181 [hep-ex/0208033] [SPIRES].

[62] BABAR collaboration, B. Aubert et al., *Measurement of the branching fraction for inclusive semileptonic B meson decays*, *Phys. Rev.* **D 67** (2003) 031101 [hep-ex/0208018] [SPIRES].

[63] S. Boutle, *Beauty in photoproduction at HERA II with the ZEUS detector*, Ph.D. Thesis, unpublished, University College London, London U.K. (2009).

[64] M. Turcato, *Measurement of beauty photoproduction at HERA*, Ph.D. Thesis, report DESY-THESIS-2003-039, Università degli Studi di Padova, Padova Italy (2003) [SPIRES].